Supporting Information for "Four decades of trends and drivers of global surface ocean acidification"

Danling Ma[1], Luke Gregor[1], and Nicolas Gruber[1]

[1]Environmental Physics, Institute of Biogeochemistry and Pollutant Dynamics, ETH Zurich, Zürich, Switzerland.

Contents of this file

1. Figures S1 to S7
2. Tables S1 to S6

Introduction This file contains additional information in support of the main paper. With regard to the tables, this files contains the details with regard to (i) the evaluation of the trends computed from the OceanSODA-ETHZ product with results from time-series sites (Table S1), (ii) mean values and long-term trends of the different parameters relevant for ocean acidification for each considered biome (Tables S2 and S3), (iii) determination of the role of the different driver mechanisms for each biome (Tables S4 and S5), and (iv) the comparison of the magnitude of the interannual variability of the OceanSODA-ETHZ product in comparison to others (Table S6). With regard to the figures, this file contains (i) maps of the components of the sDIC trends (Fig. S1), (ii) maps of the expected increases based on anthropogenic CO_2 only (Fig. S2), (iii) an error budget for the trends (Fig. S3), (iv) maps of the uncertainties in the trends based on the data uncertainties (Fig. S4), (v) maps of the trends for a wider set of parameters of relevance for ocean acidification (Fig. S5), (vi) maps of the changes in the drivers needed to assess the differerent drivers for the trends (Fig. S6), and (vii) a zonal mean plot of the lever of interannual variability of pCO_2 across different pCO_2 products (Fig. S7).

Corresponding author: Nicolas Gruber, nicolas.gruber@env.ethz.ch

Table S1. Trends for pH and Ω_{ar} (units per decade) from various sources in the literature compared with OceanSODA-ETHZ for the same periods. Note that in addition to true differences, some of these trends differ also from those computed by OceanSODA-ETHZ due to the different methods used to calculate the trends.

			pH (decade^{-1})		Ω_{ar} (decade^{-1})		
Station	Location	Period	Trend	Literature	Trend	Literature	Reference
BATS	32.0°N, 64.0°W	1983-2012	-0.014 ± 0.000	-0.017 ± 0.001	-0.066 ± 0.006	-0.095 ± 0.007	(Bates et al., 2014)
		1983-2020	-0.016 ± 0.000	-0.019 ± 0.001	-0.060 ± 0.004	-0.090 ± 0.010	(Bates & Johnson, 2020)
HOT	22.8°N, 158.0°W	1988-2007	-0.014 ± 0.001	-0.019 ± 0.002	-0.095 ± 0.013		(Dore et al., 2009)
		1988-2012	-0.015 ± 0.001	-0.016 ± 0.001	-0.098 ± 0.009	-0.084 ± 0.011	(Bates et al., 2014)
ESTOC	29.0°N, 15.5°W	1995-2012	-0.016 ± 0.001	-0.018 ± 0.002	-0.072 ± 0.014	-0.115 ± 0.023	(Bates et al., 2014)
Iceland Sea	68.0°N, 12.7°W	1983-2012	-0.019 ± 0.001	-0.014 ± 0.005	-0.056 ± 0.006	-0.018 ± 0.027	(Bates et al., 2014)
Irminger Sea	64.3°N, 28.0°W	1983-2012	-0.018 ± 0.000	-0.026 ± 0.006	-0.046 ± 0.007	-0.080 ± 0.040	(Bates et al., 2014)
Munida	45.7°S, 171.5°E	1998-2012	-0.019 ± 0.001	-0.013 ± 0.003	-0.122 ± 0.024	-0.085 ± 0.026	(Bates et al., 2014)
CARIACO	10.5°N, 64.7°W	1995-2012		-0.025 ± 0.004		-0.066 ± 0.028	(Bates et al., 2014)
137°E tropics	5-10°N, 137.0°E	1983-2017	-0.013 ± 0.000	-0.012 ± 0.008	-0.065 ± 0.005	-0.081 ± 0.050	(Ono et al., 2019)
137°E subtropics	20-22°N, 137.0°E	1983-2017	-0.016 ± 0.000	-0.017 ± 0.007	-0.080 ± 0.005	-0.113 ± 0.040	(Ono et al., 2019)
137°E Kuriosho	26-30°N, 137.0°E	1983-2017	-0.017 ± 0.001	-0.019 ± 0.008	-0.090 ± 0.006	-0.121 ± 0.050	(Ono et al., 2019)

Table S2. Trends of key variables of the ocean carbonate system for the four-decade period 1982 through 2021. All trends are reported per decade (dec^{-1}).

Region	DIC (μmol kg^{-1} dec^{-1})	fCO$_2$ (μatm dec^{-1})	[H$^+$]$_F$ (nmol kg^{-1} dec^{-1})	pH (dec^{-1})	Revelle factor (dec^{-1})	Ω_{ar} (dec^{-1})	[CO$_3^{2-}$] (μmol kg^{-1} dec^{-1})
GLOBAL	8.3 ± 0.8	16.6 ± 1.0	0.250 ± 0.016	-0.0166 ± 0.0010	0.156 ± 0.011	-0.071 ± 0.006	-4.6 ± 0.4
NP˙ICE	6.8 ± 2.2	15.7 ± 2.0	0.300 ± 0.040	-0.0200 ± 0.0040	0.250 ± 0.040	-0.050 ± 0.011	-3.4 ± 0.7
NP˙SPSS	5.4 ± 1.1	15.9 ± 1.2	0.278 ± 0.023	-0.0170 ± 0.0013	0.197 ± 0.027	-0.048 ± 0.007	-3.2 ± 0.4
NP˙STSS	8.2 ± 0.8	17.0 ± 0.8	0.258 ± 0.012	-0.0180 ± 0.0008	0.147 ± 0.012	-0.069 ± 0.006	-4.6 ± 0.4
NP˙STPS	8.1 ± 0.8	16.8 ± 0.8	0.239 ± 0.011	-0.0166 ± 0.0007	0.125 ± 0.007	-0.081 ± 0.005	-5.3 ± 0.3
PEQU˙W	9.5 ± 1.5	16.0 ± 1.1	0.212 ± 0.015	-0.0150 ± 0.0010	0.091 ± 0.009	-0.065 ± 0.008	-4.2 ± 0.5
PEQU˙E	8.8 ± 2.5	20.0 ± 2.6	0.290 ± 0.040	-0.0171 ± 0.0021	0.165 ± 0.033	-0.098 ± 0.020	-6.2 ± 1.2
SP˙STPS	8.6 ± 0.8	16.6 ± 1.0	0.243 ± 0.016	-0.0164 ± 0.0010	0.144 ± 0.011	-0.080 ± 0.007	-5.2 ± 0.4
NA˙ICE	8.0 ± 4.0	15.9 ± 1.9	0.300 ± 0.040	-0.0210 ± 0.0070	0.280 ± 0.050	-0.055 ± 0.013	-3.6 ± 0.8
NA˙SPSS	6.5 ± 1.7	15.5 ± 1.2	0.260 ± 0.023	-0.0172 ± 0.0015	0.165 ± 0.028	-0.045 ± 0.009	-3.0 ± 0.6
NA˙STSS	8.7 ± 0.7	15.7 ± 0.8	0.229 ± 0.012	-0.0161 ± 0.0008	0.132 ± 0.011	-0.065 ± 0.006	-4.3 ± 0.4
NA˙STPS	10.3 ± 0.8	16.3 ± 0.9	0.215 ± 0.013	-0.0154 ± 0.0009	0.102 ± 0.009	-0.068 ± 0.007	-4.4 ± 0.4
AEQU	6.5 ± 1.2	15.9 ± 1.1	0.219 ± 0.015	-0.0149 ± 0.0010	0.108 ± 0.011	-0.077 ± 0.009	-5.1 ± 0.5
SA˙STPS	10.8 ± 1.2	16.2 ± 0.9	0.224 ± 0.013	-0.0154 ± 0.0009	0.121 ± 0.009	-0.072 ± 0.007	-4.6 ± 0.4
IND˙STPS	8.7 ± 1.0	15.8 ± 0.9	0.221 ± 0.013	-0.0155 ± 0.0009	0.113 ± 0.009	-0.073 ± 0.007	-4.8 ± 0.4
SO˙STSS	8.1 ± 0.9	16.3 ± 0.8	0.265 ± 0.014	-0.0176 ± 0.0009	0.191 ± 0.013	-0.067 ± 0.005	-4.4 ± 0.4
SO˙SPSS	7.1 ± 0.5	17.6 ± 0.9	0.325 ± 0.017	-0.0189 ± 0.0010	0.293 ± 0.018	-0.062 ± 0.004	-4.1 ± 0.3
SO˙ICE	6.0 ± 0.6	15.0 ± 1.5	0.295 ± 0.023	-0.0165 ± 0.0013	0.282 ± 0.025	-0.049 ± 0.005	-3.3 ± 0.3

Table S3. Area weighted mean values for the parameters of the surface ocean carbonate system for each biome (Fay & McKinley, 2014) from 1982-2021.

Region	DIC (μmol kg^{-1})	Alk (μmol kg^{-1})	fCO$_2$ (μatm)	$[H^+]_F$ (nmol kg^{-1})	pH (-)	Revelle Factor (-)	Ω_{ar} (-)	Ω_{ca} (-)	$[CO_3^{2-}]$ (μmol kg^{-1})
GLOBAL	2025	2303	359	6.74	8.08	10.5	3.11	4.75	197.6
NP-ICE	2045	2204	324	7.03	8.13	14.1	1.70	2.71	111.8
NP-SPSS	2043	2218	355	7.33	8.08	13.1	1.95	3.07	127.2
NP-STSS	1991	2261	338	6.49	8.10	10.3	2.99	4.61	191.4
NP-STPS	1951	2269	357	6.50	8.08	9.3	3.59	5.44	224.4
PEQU-W	1922	2264	367	6.51	8.06	8.8	3.92	5.87	240.9
PEQU-E	1983	2281	415	7.28	8.03	9.6	3.40	5.13	212.0
SP-STPS	2022	2325	359	6.57	8.09	9.8	3.37	5.14	214.7
NA-ICE	2079	2232	299	6.61	8.14	14.1	1.69	2.70	111.7
NA-SPSS	2097	2292	334	6.84	8.11	12.5	2.13	3.35	140.2
NA-STSS	2071	2362	346	6.44	8.10	10.1	3.18	4.89	206.2
NA-STPS	2045	2391	362	6.38	8.09	9.1	3.84	5.81	244.3
AEQU	1993	2328	378	6.64	8.06	9.1	3.79	5.71	237.0
SA-STPS	2059	2380	366	6.53	8.08	9.5	3.55	5.40	227.2
IND-STPS	1971	2295	356	6.44	8.08	9.2	3.65	5.52	228.8
SO-STSS	2068	2298	339	6.70	8.11	11.4	2.51	3.92	164.2
SO-SPSS	2131	2281	358	7.52	8.08	14.2	1.68	2.67	111.0
SO-ICE	2171	2295	359	7.74	8.07	15.5	1.42	2.27	94.2

Table S4. Trends of Ω_{ar} (units per decade) decomposed into mechanisms (Mech.) for each driver. The regions are biomes from (Fay & McKinley, 2014), where the ice-covered biomes are not presented. We decompose sDIC into anthropogenic (C_{ant}) and natural (C_{nat}) components, where the latter is the residual of sDIC minus the anthropogenic component. We also show the actual trend for the variable (Trend) and the sum of the decomposed components (Σ). The mechanisms are taken from Eq 2., where m.e. indicates the mass effect.

Region	Trend	Σ	Mech.	C_{ant}	C_{nat}	sDIC	sAlk	Temp	FW
GLOBAL	-0.0711	-0.0712	ΔX	-0.0869	0.0158	-0.0711	-0.0051	0.0028	0.0020
			ω_X	-0.0039	0.0005	-0.0034	0.0000	-0.0000	-0.0000
			Ω_{ar} m.e.	0.0044	-0.0006	0.0038	-0.0001	-0.0001	0.0000
NP-SPSS	-0.0479	-0.0491	ΔX	-0.0736	0.0269	-0.0467	-0.0054	0.0022	0.0005
			ω_X	-0.0025	0.0005	-0.0019	-0.0003	-0.0000	-0.0000
			Ω_{ar} m.e.	0.0032	-0.0008	0.0024	0.0002	-0.0001	-0.0000
NP-STSS	-0.0689	-0.0697	ΔX	-0.0844	0.0243	-0.0601	-0.0167	0.0040	0.0032
			ω_X	-0.0028	0.0006	-0.0022	-0.0012	-0.0000	-0.0000
			Ω_{ar} m.e.	0.0031	-0.0007	0.0024	0.0012	-0.0001	-0.0002
NP-STPS	-0.0809	-0.0818	ΔX	-0.1074	0.0272	-0.0801	-0.0055	0.0036	0.0003
			ω_X	-0.0033	0.0003	-0.0030	-0.0007	-0.0000	-0.0000
			Ω_{ar} m.e.	0.0035	-0.0004	0.0032	0.0007	-0.0001	-0.0002
PEQU-W	-0.0647	-0.0652	ΔX	-0.0740	0.0092	-0.0648	-0.0115	0.0045	0.0069
			ω_X	-0.0035	0.0006	-0.0029	0.0000	-0.0000	-0.0000
			Ω_{ar} m.e.	0.0033	-0.0006	0.0027	-0.0000	-0.0001	-0.0000
PEQU-E	-0.0981	-0.0975	ΔX	-0.1074	0.0019	-0.1055	0.0079	0.0012	-0.0024
			ω_X	-0.0038	-0.0035	-0.0073	-0.0002	0.0000	-0.0000
			Ω_{ar} m.e.	0.0045	0.0038	0.0083	0.0002	0.0004	-0.0001
SP-STPS	-0.0795	-0.0796	ΔX	-0.0978	0.0180	-0.0798	-0.0039	0.0026	0.0014
			ω_X	-0.0038	0.0003	-0.0035	-0.0002	-0.0000	-0.0000
			Ω_{ar} m.e.	0.0042	-0.0004	0.0038	0.0002	-0.0001	-0.0001
NA-SPSS	-0.0452	-0.0457	ΔX	-0.0635	0.0261	-0.0374	-0.0139	0.0032	0.0023
			ω_X	-0.0027	0.0008	-0.0019	-0.0002	-0.0000	-0.0000
			Ω_{ar} m.e.	0.0034	-0.0010	0.0024	-0.0001	-0.0001	-0.0000
NA-STSS	-0.065	-0.0652	ΔX	-0.0873	0.0229	-0.0644	-0.0078	0.0037	0.0035
			ω_X	-0.0033	0.0009	-0.0024	-0.0002	-0.0000	-0.0000
			Ω_{ar} m.e.	0.0034	-0.0009	0.0025	0.0002	-0.0002	-0.0001
NA-STPS	-0.0676	-0.0673	ΔX	-0.0842	0.0103	-0.0739	-0.0033	0.0044	0.0057
			ω_X	-0.0034	0.0007	-0.0027	0.0000	-0.0000	-0.0000
			Ω_{ar} m.e.	0.0034	-0.0007	0.0027	-0.0000	-0.0001	-0.0001
AEQU	-0.0774	-0.0783	ΔX	-0.1254	0.0393	-0.0862	0.0074	0.0039	-0.0036
			ω_X	-0.0055	0.0023	-0.0032	0.0006	-0.0000	-0.0000
			Ω_{ar} m.e.	0.0059	-0.0024	0.0034	-0.0007	-0.0002	0.0003
SA-STPS	-0.0719	-0.071	ΔX	-0.0621	-0.0018	-0.0640	-0.0172	0.0025	0.0076
			ω_X	-0.0049	0.0015	-0.0034	0.0003	-0.0000	0.0000
			Ω_{ar} m.e.	0.0049	-0.0015	0.0034	-0.0003	-0.0001	0.0002
IND-STPS	-0.0734	-0.0737	ΔX	-0.0940	0.0205	-0.0735	-0.0064	0.0035	0.0026
			ω_X	-0.0047	0.0013	-0.0033	0.0002	-0.0000	0.0000
			Ω_{ar} m.e.	0.0048	-0.0013	0.0034	-0.0002	-0.0001	0.0001
SO-STSS	-0.0667	-0.0664	ΔX	-0.0771	0.0155	-0.0616	-0.0095	0.0021	0.0021
			ω_X	-0.0047	0.0008	-0.0039	0.0004	-0.0000	-0.0000
			Ω_{ar} m.e.	0.0055	-0.0009	0.0046	-0.0006	-0.0001	0.0001
SO-SPSS	-0.0616	-0.0605	ΔX	-0.0707	0.0033	-0.0674	0.0058	0.0004	-0.0006
			ω_X	-0.0041	0.0002	-0.0040	0.0008	-0.0000	-0.0000
			Ω_{ar} m.e.	0.0058	-0.0002	0.0055	-0.0011	-0.0000	0.0001

Table S5. The same as Table S4 but for $[H^+]$ in nmol · kg-1 · decade-1.

Region	Trend	Σ	Mech.	C^{ant}	C^{nat}	sDIC	sAlk	Temp	FW
GLOBAL	0.2502	0.2853	ΔX	0.2510	-0.0438	0.2073	0.0106	0.0381	0.0037
			β_X	0.0083	-0.0010	0.0073	-0.0003	-0.0000	-0.0000
			$[H^+]$ m.e.	0.0195	-0.0025	0.0170	-0.0003	0.0019	0.0000
NP-SPSS	0.2777	0.314	ΔX	0.3274	-0.1165	0.2109	0.0171	0.0561	0.0012
			β_X	0.0085	-0.0020	0.0066	0.0009	-0.0000	-0.0001
			$[H^+]$ m.e.	0.0201	-0.0045	0.0156	0.0021	0.0033	0.0003
NP-STSS	0.2575	0.3006	ΔX	0.2333	-0.0695	0.1638	0.0418	0.0601	0.0071
			β_X	0.0054	-0.0012	0.0042	0.0026	-0.0000	-0.0001
			$[H^+]$ m.e.	0.0130	-0.0026	0.0104	0.0061	0.0036	0.0010
NP-STPS	0.2392	0.274	ΔX	0.2543	-0.0634	0.1910	0.0135	0.0449	0.0011
			β_X	0.0050	-0.0004	0.0045	0.0013	-0.0000	-0.0001
			$[H^+]$ m.e.	0.0126	-0.0011	0.0115	0.0029	0.0026	0.0008
PEQU-W	0.2124	0.2477	ΔX	0.1673	-0.0208	0.1464	0.0217	0.0512	0.0114
			β_X	0.0049	-0.0008	0.0040	-0.0000	-0.0000	-0.0001
			$[H^+]$ m.e.	0.0145	-0.0026	0.0119	-0.0001	0.0012	0.0001
PEQU-E	0.2852	0.3278	ΔX	0.3000	-0.0031	0.2969	-0.0188	0.0159	-0.0055
			β_X	0.0080	0.0064	0.0144	0.0002	0.0000	-0.0000
			$[H^+]$ m.e.	0.0169	0.0144	0.0313	0.0006	-0.0076	0.0004
SP-STPS	0.2427	0.2744	ΔX	0.2540	-0.0460	0.2080	0.0063	0.0336	0.0021
			β_X	0.0070	-0.0006	0.0064	0.0002	-0.0000	-0.0000
			$[H^+]$ m.e.	0.0164	-0.0016	0.0148	0.0006	0.0021	0.0003
NA-SPSS	0.2604	0.2973	ΔX	0.2321	-0.0992	0.1329	0.0545	0.0738	0.0085
			β_X	0.0077	-0.0024	0.0053	0.0006	-0.0000	-0.0001
			$[H^+]$ m.e.	0.0185	-0.0064	0.0121	0.0030	0.0062	0.0005
NA-STSS	0.229	0.2634	ΔX	0.2281	-0.0602	0.1678	0.0172	0.0500	0.0067
			β_X	0.0059	-0.0016	0.0043	0.0005	-0.0000	-0.0000
			$[H^+]$ m.e.	0.0151	-0.0042	0.0109	0.0011	0.0045	0.0004
NA-STPS	0.2155	0.2488	ΔX	0.1870	-0.0229	0.1641	0.0064	0.0506	0.0095
			β_X	0.0048	-0.0009	0.0039	-0.0000	-0.0000	-0.0001
			$[H^+]$ m.e.	0.0137	-0.0025	0.0112	0.0000	0.0029	0.0003
AEQU	0.2187	0.2457	ΔX	0.2923	-0.0906	0.2017	-0.0143	0.0470	-0.0062
			β_X	0.0082	-0.0034	0.0048	-0.0010	-0.0000	-0.0000
			$[H^+]$ m.e.	0.0222	-0.0092	0.0129	-0.0021	0.0039	-0.0010
SA-STPS	0.2241	0.2563	ΔX	0.1496	0.0041	0.1537	0.0366	0.0316	0.0141
			β_X	0.0080	-0.0024	0.0056	-0.0006	-0.0000	0.0000
			$[H^+]$ m.e.	0.0199	-0.0060	0.0139	-0.0011	0.0030	-0.0005
IND-STPS	0.2208	0.2527	ΔX	0.2196	-0.0474	0.1723	0.0133	0.0426	0.0049
			β_X	0.0071	-0.0021	0.0051	-0.0003	-0.0000	0.0000
			$[H^+]$ m.e.	0.0191	-0.0055	0.0136	-0.0007	0.0023	-0.0004
SO-STSS	0.2654	0.303	ΔX	0.2559	-0.0500	0.2060	0.0244	0.0380	0.0050
			β_X	0.0119	-0.0019	0.0100	-0.0014	-0.0000	-0.0000
			$[H^+]$ m.e.	0.0258	-0.0041	0.0217	-0.0024	0.0021	-0.0004
SO-SPSS	0.325	0.3656	ΔX	0.3584	-0.0165	0.3419	-0.0256	0.0121	-0.0023
			β_X	0.0168	-0.0007	0.0160	-0.0031	-0.0000	-0.0000
			$[H^+]$ m.e.	0.0345	-0.0018	0.0327	-0.0058	0.0004	-0.0007

Table S6. Comparison of interannual variability among seven pCO_2 products from the lowest to highest relative to OceanSODA-ETHZ: OceanSODA-ETHZ (Gregor & Gruber, 2021), CSIR-ML6 version 2019a (Gregor et al., 2019), CMEMS-FFNN (Denvil-Sommer et al., 2019), NIES-FNN (Zeng et al., 2015), MPI-SOMFFN (Landschützer et al., 2016), JMA-MLR (Iida et al., 2021), and Jena-MLS (Rödenbeck et al., 2013). Interannual variability in other data sets is scaled proportionally to that of OceanSODA-ETHZ, which is set to 1 by default.

Product	Scaled interannual variability
OceanSODA-ETHZ	1.00
CSIR-ML6 version 2019a	1.10
CMEMS-FFNN	1.31
NIES-FNN	1.56
MPI-SOMFFN	2.14
JMA-MLR	2.36
Jena-MLS	3.21

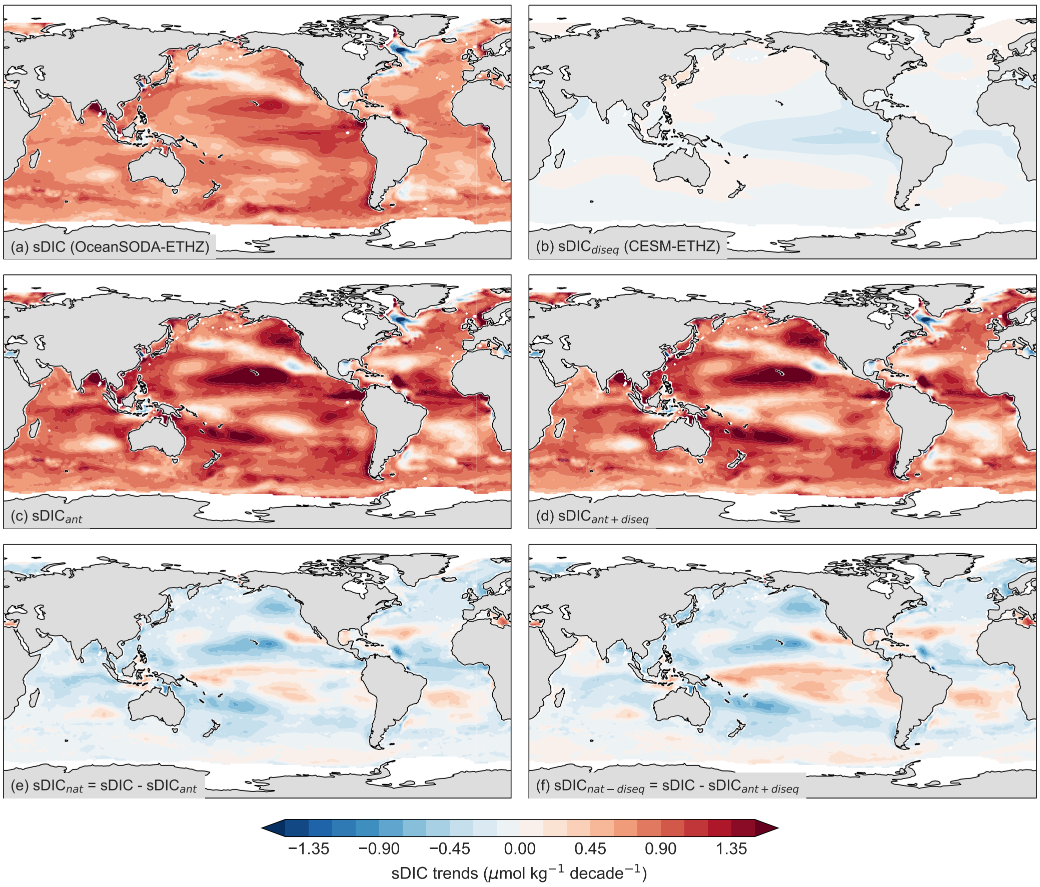

Figure S1. Maps of the trends of salinity normalized DIC (sDIC) and of its components for the period 1982 through 2021. (a) sDIC trends based on OceanSODA-ETHZ (Gregor & Gruber, 2021) (b) Trends in the disequilibrium term of anthropogenic CO2, i.e., C_{ant}^{dis-eq}, calculated from simulations with the CESM-ETHZ model. (c) Trend in surface ocean anthropogenic CO2 if it followed the atmospheric perturbation perfeclty, i.e., the equilibrium component of C_{ant}, C_{ant}^{eq}, computed from the change in atmospheric pCO_2. (d) Expected trend in surface ocean anthropogenic CO2, taking into account the disequilibrium term, i.e., $C_{ant} = C_{ant}^{eq}$ - C_{ant}^{dis-eq}. (e) The trend of the natural sDIC component without the disequilibrium term of C_{ant}, calculated by the residual of the trends in sDIC (panel a), and the trends in C_{ant}^{eq} (panel c), i.e., C'_{nat} = sDIC - C_{ant}^{eq}. (f) The trend of the natural sDIC component including the disequilibrium term of C_{ant} calculated as C_{nat} = sDIC - C_{ant}, i.e., (panel a) - (panel d).

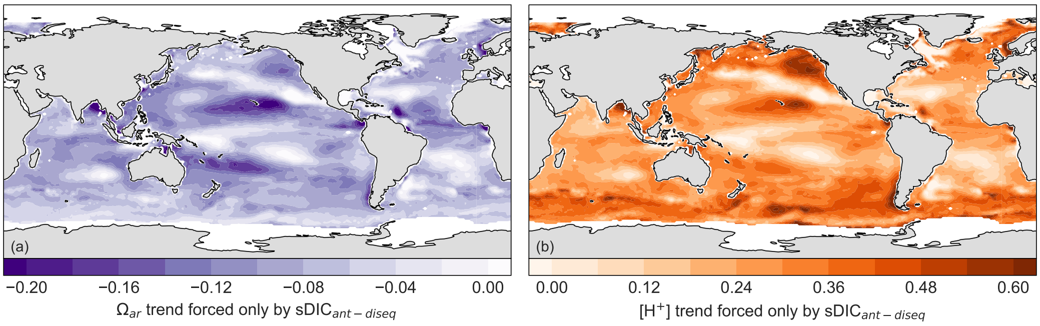

Figure S2. Expected increases in (a) Ω_{ar} and (b) $[H^+]_F$ due to the accumulation of anthropogenic CO2 only, i.e., the increase in $C_{ant} = C^{eq}_{ant}$ - C^{dis-eq}_{ant}. (shown in Figure S1d).

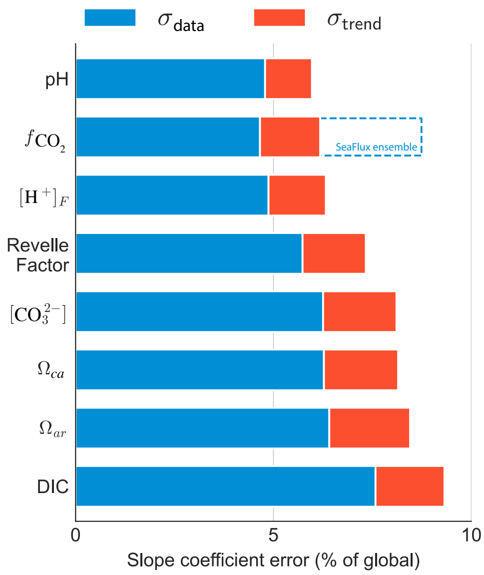

Figure S3. Contribution of the different sources of error to the total error of the trend. Shown are the two considered components, i.e., the error of the trend, σ_{trend} (red) and the error of the underlying data, σ_{data}. The latter is estimated through an ensemble approach. Also shown as a blue dashed line is the estimated trend uncertainty for fCO_2 based on the SeaFlux ensemble. See main text for further details.

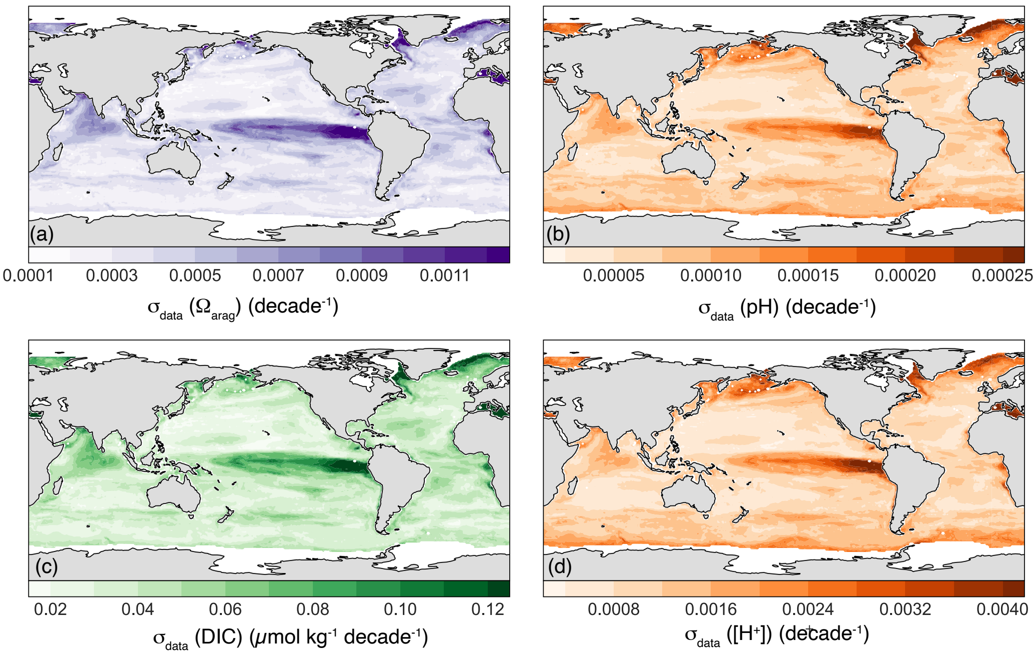

Figure S4. Map of the data-driven uncertainty of the long-term trend, i.e., the magnitude of σ_{data}. Data-driven trend uncertainty for (a) Ω_{ar}, (b) pH, (c) DIC, and (d) $[\text{H}^+]_F$.

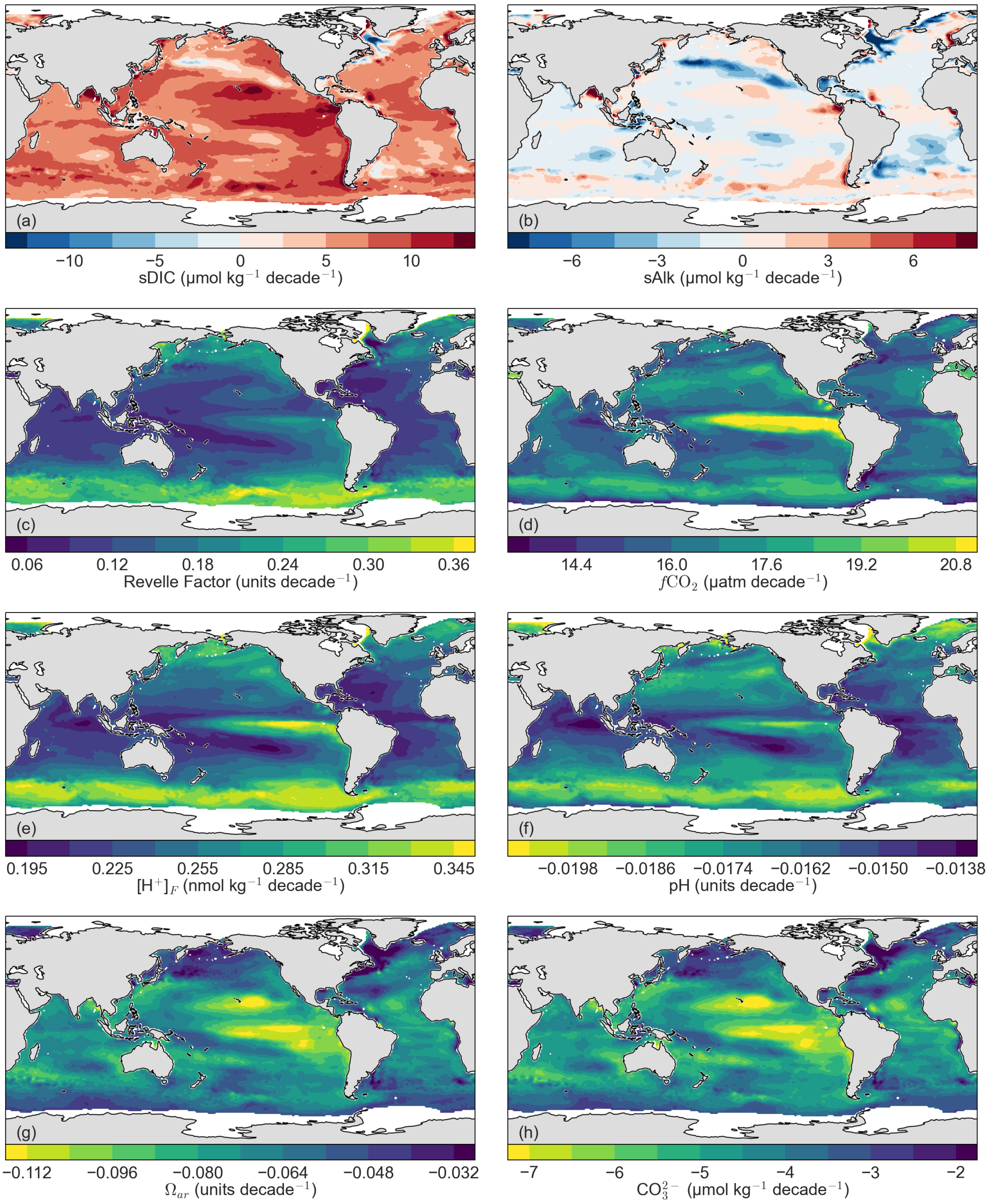

Figure S5. Maps depicting the average trends of (a) sDIC, (b) sAlk, (c) Revelle factor, (d) fCO2, (e) $[H^+]_F$, (f) pH, (g) Ω_{ar}, and (h) $[CO_3^{2-}]$ from 1982 to 2021.

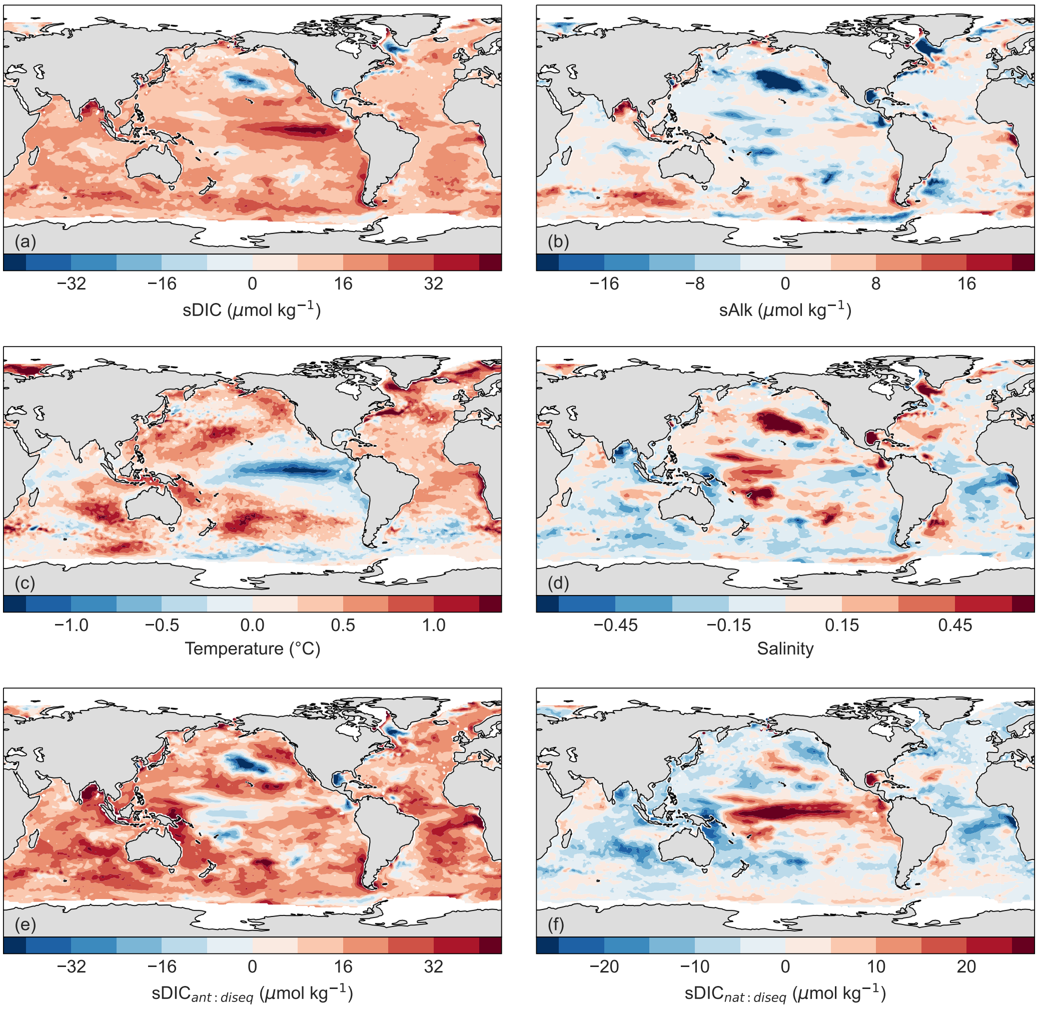

Figure S6. Maps showing the mean change (ΔX in Eq 2 and 3) in (a) sDIC, (b) sAlk, (c) temperature, (d) freshwater input, (e) sDIC$_{ant:diseq}$, and (f) sDIC$_{nat:diseq}$ from 1982 to 2021. Note that the mean change is calculated with $\Delta X = \sum_{i=1}^{N}(X_i - X_0)/N$ where X is the driver, i is the time step (years), X_0 is the first time step in X and N is the total number of years (40). The pattern of the mean changes differ somewhat from the mapped trends shown in Figure S5, since it includes all temporal changes, while the trends just the depict the slopes of the linear regression, i.e., does not include the residuals.

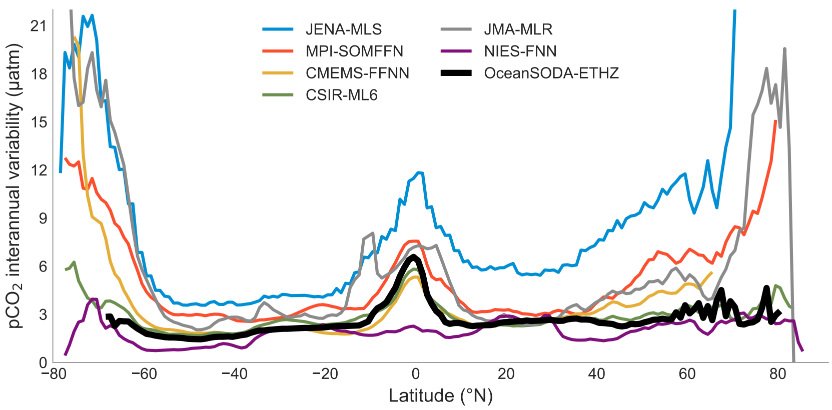

Figure S7. Comparison of zonally averaged interannual variability of pCO_2 for the seven pCO_2 products shown in Table S6.

References

Bates, N. R., Astor, Y. M., Church, M. J., Currie, K., Dore, J. E., González-Dávila, M., … Santana-Casiano, J. M. (2014). A time-series view of changing surface ocean chemistry due to ocean uptake of anthropogenic CO_2 and ocean acidification. *Oceanography*, *27*(1), 126–141.

Bates, N. R., & Johnson, R. J. (2020). Acceleration of ocean warming, salinification, deoxygenation and acidification in the surface subtropical north atlantic ocean. *Communications Earth & Environment*, *1*(1), 33.

Denvil-Sommer, A., Gehlen, M., Vrac, M., & Mejia, C. (2019). Lsce-ffnn-v1: a two-step neural network model for the reconstruction of surface ocean pco 2 over the global ocean. *Geoscientific Model Development*, *12*(5), 2091–2105.

Dore, J. E., Lukas, R., Sadler, D. W., Church, M. J., & Karl, D. M. (2009). Physical and biogeochemical modulation of ocean acidification in the central North Pacific. *Proceedings of the National Academy of Sciences*, *106*(30), 12235–12240.

Fay, A., & McKinley, G. (2014). Global open-ocean biomes: mean and temporal variability. *Earth System Science Data*, *6*(2), 273–284.

Gregor, L., & Gruber, N. (2021). OceanSODA-ETHZ: a global gridded data set of the surface ocean carbonate system for seasonal to decadal studies of ocean acidification. *Earth System Science Data*, *13*(2), 777–808.

Gregor, L., Lebehot, A. D., Kok, S., & Scheel Monteiro, P. M. (2019). A comparative assessment of the uncertainties of global surface ocean CO_2 estimates using a machine-learning ensemble (CSIR-ML6 version 2019a)–have we hit the wall? *Geoscientific Model Development*, *12*(12), 5113–5136.

Iida, Y., Takatani, Y., Kojima, A., & Ishii, M. (2021). Global trends of ocean CO_2 sink and ocean acidification: an observation-based reconstruction of surface ocean inorganic carbon variables. *Journal of Oceanography*, *77*(2), 323–358.

Landschützer, P., Gruber, N., & Bakker, D. C. (2016). Decadal variations and trends of the global ocean carbon sink. *Global Biogeochemical Cycles*, *30*(10), 1396–1417.

Ono, H., Kosugi, N., Toyama, K., Tsujino, H., Kojima, A., Enyo, K., … Ishii, M. (2019). Acceleration of Ocean Acidification in the Western North Pacific. *Geophysical Research Letters*, *46*(22), 13161–13169. doi: 10.1029/2019GL085121

Rödenbeck, C., Keeling, R. F., Bakker, D. C., Metzl, N., Olsen, A., Sabine, C., & Heimann, M. (2013). Global surface-ocean pCO_2 and sea–air CO_2 flux variability from an observation-driven ocean mixed-layer scheme. *Ocean Science*, *9*(2), 193–216.

Zeng, J., Nojiri, Y., Nakaoka, S.-i., Nakajima, H., & Shirai, T. (2015). Surface ocean CO_2 in 1990–2011 modelled using a feed-forward neural network. *Geoscience Data Journal*, *2*(1), 47–51.